New slip rate estimates for the creeping segment of the San Andreas fault, California

Sarah J. Titus
Charles DeMets
Basil Tikoff
Department of Geology and Geophysics, University of Wisconsin, Madison, Wisconsin 53706, USA

ABSTRACT

New continuous and differential global positioning system (GPS) measurements of recent slip rates and 30 yr alignment-array offsets from the central creeping segment of the San Andreas fault yield a maximum right-lateral slip rate of 25 ± 1 mm/yr. This slip rate is 20% slower than the 30 mm/yr slip rate accepted for this segment of the fault and 35% slower than the 39 mm/yr slip rate predicted between the Sierra Nevada–Great Valley block and the Pacific plate. New continuous GPS measurements between pairs of sites that flank the creeping segment at intersite distances of 1.0 km and 70 km give relative fault-parallel slip rates of 28 ± 2 and 30 ± 2 mm/yr, respectively. These observations indicate that right-lateral deformation rates increase with distance from the fault. Possible explanations for the gradient observed in the geodetic data are elastic strain accumulation along the creeping segment or significant distributed deformation on off-fault structures.

Keywords: San Andreas fault, global positioning system, creep, elastic strain, deformation.

INTRODUCTION

The creeping segment of the San Andreas fault is understudied compared to other sections of the fault because of its sparse population and perceived low seismic hazard. The 175-km-long creeping segment, which extends from San Juan Bautista to Cholame, separates locked sections of the fault to the southeast and northwest that ruptured during the earthquakes of 1857 and 1906, respectively. Movement on this part of the fault is characterized by aseismic slip (creep) and the occurrence of shallow (<15 km depth) microearthquakes (e.g., Hill et al., 1990).

We present results of new global positioning system (GPS)–based slip rates on the central creeping segment with 30 yr rates derived from differential GPS measurements at preexisting U.S. Geological Survey (USGS) alignment arrays and 1.5 yr estimates from 4 new continuous GPS sites. The revised rates, which agree well with creepmeter rates (e.g., Schulz et al., 1982; Schulz, 1989) and rates we reinterpret from 10 yr USGS alignment-array surveys (Burford and Harsh, 1980), suggest that the San Andreas fault accommodates 25 ± 1 mm/yr of right-lateral slip. This rate is slower than the frequently cited 30 mm/yr slip rate for the creeping segment (Burford and Harsh, 1980) and the 34–40 mm/yr rate estimated from trilateration networks, very long baseline interferometry, satellite laser ranging, and far-field GPS (e.g., Savage and Burford, 1973; Lisowski et al., 1991; Argus and Gordon, 2001), which measure rates at significantly greater distances from the fault trace. The discrepancy between the near-field and far-field geodetic rates implies that seismic hazards may be greater than previously thought along this section of the fault.

DATA ANALYSIS

From 1967 to 1970, workers at the USGS installed 25 sets of originally linear, fault-perpendicular benchmarks along the creeping segment. These alignment arrays range from 30 to 200 m in length and were surveyed several times with theodolites to measure 10 yr creep rates along the fault. The highest rates were documented along the 55-km-long central creeping segment; the rates decreased to the northwest and southeast toward the locked segments (Burford and Harsh, 1980).

In 2003, we used differential GPS to survey 3 alignment arrays for the first time in 25 yrs (Figs. 1 and 2A). Monuments are all standard USGS brass benchmarks either set directly into concrete postholes or freely moving inside transite pipes. Each monument was occupied with a dual-frequency Trimble 5700 and a Zephyr geodetic antenna generally for 20–30 min and as long as 24 h. Differential processing with Trimble's GPSurvey software was used to establish the location of each marker relative to the location of a continuously operating GPS receiver within or near the array. A detailed analysis of the repeatability of the relative site locations through time, with respect to the base station, indicates that the north and east baseline components are repeatable (at the 2σ level) for consecutive 20 min intervals at the ±5 mm level.

We estimated fault offsets and hence slip rates from the relative site locations as follows. The north and east coordinates of each site location and the associated covariances

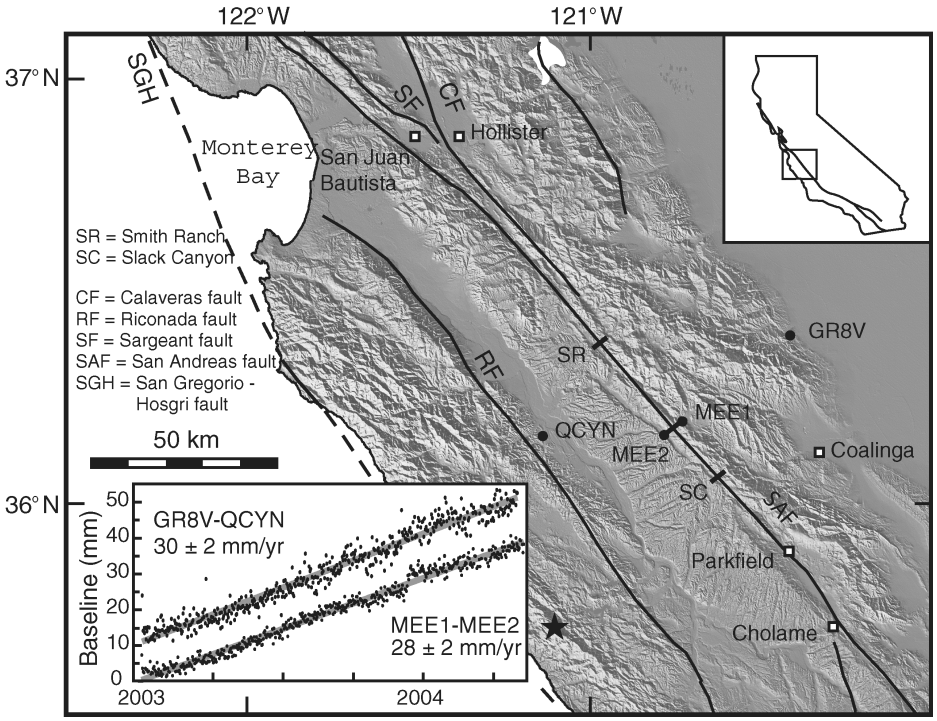

Figure 1. Map of creeping segment of San Andreas fault, showing location of alignment arrays (dark bars), continuous global positioning system stations (black dots), and 2003 San Simeon earthquake (star). Inset shows rate of change of horizontal baseline for site MEE2 relative to site MEE1 and for site QCYN relative to site GR8V.

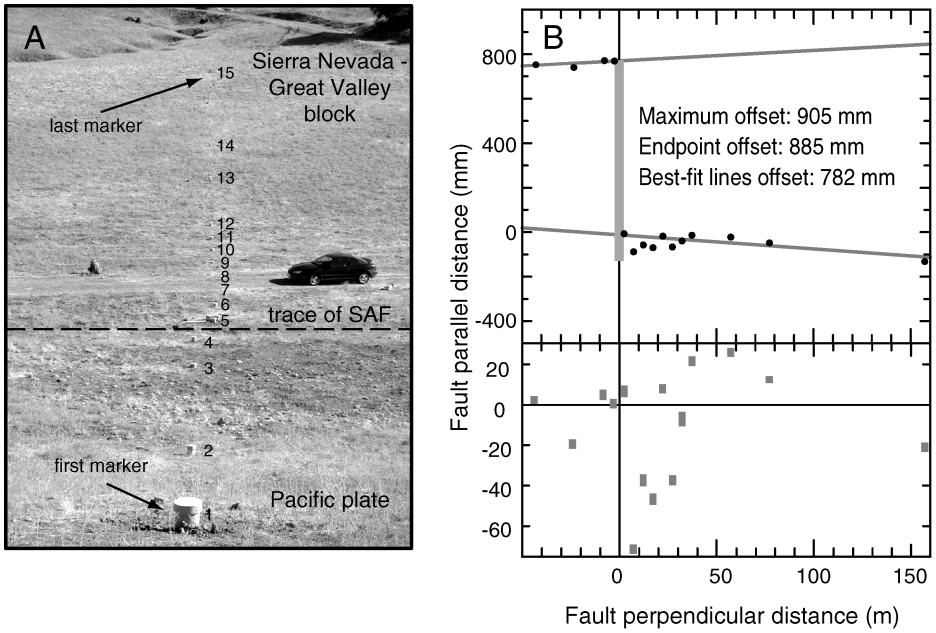

Figure 2. A: Photograph of Mee Ranch alignment array looking northeast; numbers are located to right of monuments. Car for scale. B: Example of alignment-array offset analysis from Mee Ranch. Upper panel shows monument locations in fault-centered reference frame. *Y*-axis represents local trace of San Andreas fault (SAF). Best-fit lines are shown for monuments on each side of fault; vertical gray bar represents maximum offset. Lower panel shows residuals from best-fit lines plus 1σ uncertainties propagated from location covariances.

were first rotated into a fault-centered reference frame. For each alignment array, a linear regression of the rotated site coordinates and covariances was used to obtain best-fitting slopes for monuments on either side of the fault and the slope intercept at the fault location (Fig. 2). The total offsets, in a fault-centered reference frame, were determined by (1) the difference in intercept values, (2) the difference in the endpoint values, and (3) the maximum offset of any two monuments. The slip rates determined from these offsets are shown in Table 1. We did a rate sensitivity analysis to reestimate fault offsets, while omitting various subsets of sites based on their stabilities, and found that the slip rates were generally insensitive to the subset of site locations inverted at the 1 mm/yr level and often at the 0.5 mm/yr level.

The mean departure of the monument locations from their best-fit lines is 15 mm, but range from 0 to 70 mm (Fig. 2). These misfits are much greater than the uncertainty in the relative site locations. We observe no obvious pattern to the misfits, indicating that each alignment array is offset along a single fault. Our field observations suggest that the large residuals are caused by geologic ''noise,'' consistent with the magnitude expected from instability induced by changes in precipitation, slope stability, and soil creep (e.g., Yamada, 1999). Examination of Burford's original notes (J. Langbein) indicates that 10–20 mm residuals were common in the original 10 yr observations.

Four continuously recording GPS sites were also used in this analysis (Fig. 1). Two near-fault sites, MEE1 and MEE2, are 1.0 km apart and span the fault near the Mee Ranch alignment array. Sites QCYN and GR8V are located 44 km northeast and 42 km southwest of the fault, respectively, but do not form a perfect fault-perpendicular transect and are 70 km apart across the San Andreas fault. Continuous code-phase GPS measurements from all four sites were analyzed by using GIPSY analysis software (Zumberge et al., 1997), precise satellite orbits and clocks from the Jet Propulsion Laboratory (Pasadena, California), and a point-positioning analysis strategy that includes resolution of phase ambiguities. Daily GPS station coordinates are estimated in a no-fiducial reference frame (Heflin et al., 1992) and then transformed to ITRF2000 (Altamimi et al., 2002). The daily scatters of the coordinates for all 4 sites relative to their 30 day mean locations are 1–3 mm, typical for continuous GPS sites.

RESULTS

The slip rates we derived from the best-fit, endpoint, and maximum offset analyses of the three alignment-array surveys are shown in Table 1. The best-fit rates employ most or all of the monument locations to estimate the array offsets and are thus likely to be the most robust estimates of the fault-slip rate. Rates based on the maximum monument offsets are more likely to be influenced by residual errors for individual monuments (which can change the slip rate by ±1 mm/yr) and are thus primarily useful for establishing an upper bound on the slip rate. The 30 yr best-fit and endpoint rates for both the Smith Ranch and Mee Ranch alignment arrays agree well with each other, but are 2–4 mm/yr faster than the more uncertain 30 yr slip rate for the Slack Canyon array, which has fewer monuments and is shorter than the other two alignment arrays. On the basis of the slip rates for the Mee and Smith Ranch arrays, we estimate an average slip rate of 25 mm/yr on the central creeping segment; the approximate uncertainties of ±1 mm/yr are based on the sensitivity analysis of each array.

The 25 ± 1 mm/yr slip rate we find for the central San Andreas fault is significantly slower than the 30–33 mm/yr slip rates derived by Burford and Harsh (1980, see their Fig. 10) from the offsets of the endpoints of their alignment arrays, but agrees better with their slower best-fitting rates (Table 1; Fig. 3). Long-term creepmeter measurements at the Smith Ranch and Slack Canyon sites support the slower rate. Simple regressions of the 12-yr-long and 34-yr-long creepmeter time series from these two sites yield slip rates of 26.5 and 22.0 mm/yr (Fig. 3), respectively, the same within errors as the rates derived from

TABLE 1. ALIGNMENT-ARRAY DATA FOR THE CENTRAL CREEPING SEGMENT OF THE SAN ANDREAS FAULT

Site name	Lat (°N)	Long (°W)	Survey dates*		10 yr slip rates		30 yr slip rates		
			DFS	DLS	BF	EP	BF	EP	Max
Smith Ranch	36.3883	120.969	67:238	03:299	22.1	33.3	26.2	23.2	27.6
Mee Ranch	36.1800	120.798	70:238	03:299	26.5	26.0	23.6:24.6	26.7:24.1	27.3:25.3
Slack Canyon	36.0650	120.628	68:045	03:300	23.9	30.0	21.2	22.2	24.3
Average					24.2	29.8	23.7	24.0	26.4
Average†							24.9:25.4	24.9:23.7	27.5:26.5

Note: Abbreviations used: DFS and DLS—dates of first survey (Buford and Harsh, 1980) and last survey (ours), respectively. BF—average slip rate between first and last surveys based on fault offset determined by best-fit lines. EP—average slip rate between first and last surveys based on offset of array endpoints. Max—average slip rate based on greatest offset between any two monuments. Two rates cited for Mee Ranch reflect inclusion (first number) and exclusion (second number) of North American monument farthest from fault in rate analysis (see monument 15 in Fig. 2A).

*Given as year: Julian day.

†Average reflects average of values from Smith Ranch and first set of rate estimates from Mee Ranch followed by the average based on second set of values from Mee Ranch. See Figure 2 and text for details.

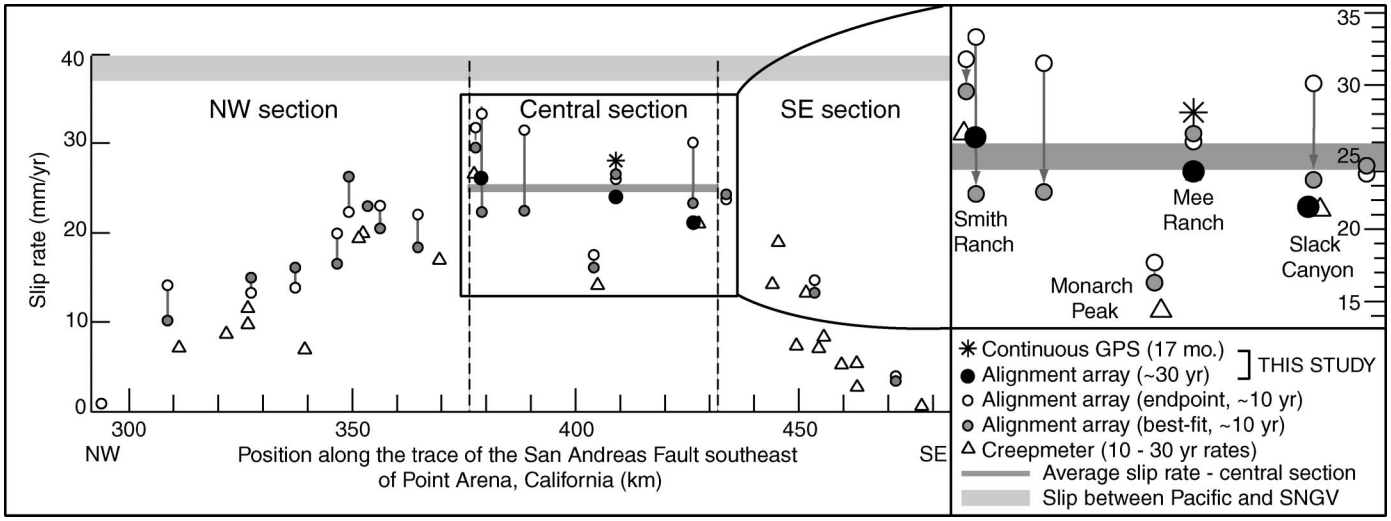

Figure 3. Distribution of slip rates along creeping segment of San Andreas fault, modified from Burford and Harsh (1980). Circles represent slip rates determined from alignment-array surveys; white and gray circles show different analyses of Burford and Harsh (1980). 30 yr alignment rates are best-fitting rates from Table 1. All creepmeter rates are from Schulz (1989), except at Smith Ranch (Schulz et al., 1982) and Slack Canyon (our analyses). Inset shows data for central creeping segment in expanded scale. Sierra Nevada–Great Valley (SNGV) block to Pacific plate rate (upper shaded area) is estimated from Argus and Gordon (2001). Pacific—Pacific plate; GPS—global positioning system.

our alignment measurements (creepmeter data are from Schulz [1989], and the USGS Web site). Although the creepmeters measure slip across a narrower zone (~2 m) compared to the alignment arrays, they nonetheless yield remarkably similar slip rates. Given these constraints, we take 25 ± 1 mm/yr as a measure of the rate of surficial transcurrent motion on the San Andreas fault proper.

The motions of GPS sites MEE2 relative to MEE1 and QCYN relative to GR8V record deformation over increasingly larger distances from the San Andreas fault (Fig. 1) and thus provide useful new information about the fault-normal deformation gradient along the central creeping segment. Relative to MEE1, site MEE2 moves northwestward at 28 ± 2 mm/yr parallel to the San Andreas fault, slightly faster than the 25 ± 1 mm/yr fault-centered slip derived from the Mee Ranch alignment array. Relative to GR8V, site QCYN moves 30 ± 2 mm/yr northwestward parallel to the San Andreas fault. Although the coordinate time series from all 4 sites are still relatively short (17 months) and are thus susceptible to long-period noise, much of the daily noise and some of the longer-period noise present in their raw time series is strongly correlated and hence cancels when their individual coordinate time series are differenced. The resulting relative coordinate time series are remarkably linear (Fig. 1) and yield relative site movements parallel to both the San Andreas fault and the relative motion between the Sierra Nevada–Great Valley block and the Pacific plate. Fault-parallel motion of 28 ± 2 mm/yr between sites MEE1 and MEE2 is the same within uncertainties as measured by older trilateration measurements for the Mee Ranch net (Lisowski and Prescott, 1981), which sample deformation over a comparable scale.

In summary, motion between sites at varying distances from the San Andreas fault increases away from the fault: 25 ± 1 mm/yr at the fault, 28 ± 2 mm/yr at 1 km distance, and 30 ± 2 mm/yr at 70 km distance. At even greater distances, the angular velocity that best describes motion of the Sierra Nevada–Great Valley block relative to the Pacific plate predicts a rate of 39 ± 2 (95%) mm/yr across the entire deforming zone (Argus and Gordon, 2001).

DISCUSSION

The 25 ± 1 mm/yr steady slip rate we determined for the central creeping segment is 14 ± 2 mm/yr slower than the 39 ± 2 mm/yr deformation rate predicted for lithosphere west of the Great Valley (Argus and Gordon, 2001) and 9 ± 3 mm/yr slower than the widely cited geologic estimate of 34 ± 3 mm/yr, based on Holocene offsets at Wallace Creek (Sieh and Jahns, 1984). The discrepancy between geodetic and paleoseismologic slip rates implies that seismic hazards on or near the central creeping segment may be greater than previously recognized.

Two end-member models offer a useful framework for explaining the observed slip deficit. In one model, the creeping segment accommodates the total plate motion and the missing slip is attributed to elastic strain. Alternatively, the geodetic slip rate represents the long-term slip rate and the missing slip is accommodated by deformation on off-fault structures. We discuss these hypotheses in greater detail, including the seismic hazards implied by each model.

A model in which the slip deficit is accommodated by elastic strain as a result of frictional locking of the creeping segment is consistent with historical evidence for moderate-sized earthquakes ($M > 5.5$) in the late 1800s that may have ruptured the creeping segment between Parkfield and San Juan Bautista (Toppozada et al., 2002). If we assume that an elastic slip deficit of 14 mm/yr has accrued since the last major historical earthquake in this area, recovery of the entire ~1.4 m slip deficit during a single future rupture of a deeply locked patch extending along the 55-km-long central creeping segment would produce an earthquake of $M_w \approx 6.7$. This magnitude is a likely upper bound because it assumes that all of the elastic strain would be released in a single event.

Geodetic site velocities and creep rates have been used to infer the existence of a deeply locked seismogenic zone along the San Andreas fault near Parkfield (King et al., 1987; Segall and Harris, 1987) and north of San Francisco (Prescott et al., 2001), and Lienkaemper et al. (1991) interpreted systematic variations in surficial creep rates as evidence for a deeply locked seismogenic zone along the Hayward fault. Each of these areas may serve as useful analogs for the central creeping segment. A simple elastic model, assuming 39 mm/yr of fault-parallel slip with deep locking from 10–15 km, produces a strain gradient consistent with that observed in our geodetic data. Elastic locking of deep areas of the fault could also explain why the present slip rate is slower than the 34 ± 3 mm/yr long-term slip rate for the San Andreas fault along the Carrizo Plain.

An alternative end-member model assumes that the 25 ± 1 mm/yr surficial slip rate along the creeping segment represents the long-term

and hence deep slip rate. Such a model implies that the 14 ± 2 mm/yr slip deficit, representing 35% of the total motion between the Pacific plate and Sierra Nevada–Great Valley block, is accommodated by deformation on structures adjacent to the San Andreas fault, including subparallel faults and the borderlands between the major faults. Furthermore, a surprisingly large fraction of the total plate motion (9 ± 3 mm/yr) is accommodated by structures that are more than 35 km away from the San Andreas fault. This model implies that structures adjacent to the San Andreas fault may pose a larger seismic hazard than currently anticipated, as illustrated by the 2003 M = 6.5 San Simeon earthquake (Fig. 1).

A variety of geologic and geophysical observations support the idea of distributed deformation in western California. First, significant dextral strike-slip movement has occurred on subparallel faults southwest of the San Andreas fault. Clark et al. (1984) estimated 160 km of offset along the San Gregorio–Hosgri fault, geologic studies of the San Simeon fault zone in this region estimated 1–3 mm/yr of slip (Hall et al., 1994; Hanson and Lettis, 1994), and there is evidence for 60 km of dextral offset along the Rinconada fault (Dibblee, 1976). Second, many earthquakes in the borderlands display oblique-slip first-motion focal mechanisms (e.g., Fig. 9 in McLaren and Savage, 2001), indicating that faults accommodate both fault-normal and fault-parallel deformation over a broad region in central California. Third, folding in the Coast Ranges (e.g., Page et al., 1998), which reflects permanent deformation in the borderlands over geologic time scales, can accommodate some of the total transcurrent motion (Jamison, 1991; Teyssier and Tikoff, 1998; Tikoff and Peterson, 1998). By using a transpressional kinematic model and balanced cross sections, Teyssier and Tikoff (1998) estimated that as much as 13 mm/yr of tangential motion can be accommodated by distributed deformation in the borderlands. This estimate, combined with the 25 ± 1 mm/yr that we observe on the San Andreas fault, can account for the total transcurrent component of plate motion.

In reality, the slip-rate deficit may best be explained by some combination of the elastic and permanent deformation models. Testing the two end-member models will, as always, be challenging. Locking along deeper parts of the fault accompanied by creep along shallower areas of the fault should give rise to predictable geodetic velocity gradients that are symmetric or nearly symmetric with respect to the fault (depending on whether the bulk crustal material properties on either side of the fault differ significantly). Evidence for highly asymmetric velocity gradients relative to the fault, possibly accompanied by identifiable velocity gradients associated with off-fault structures, would constitute useful evidence for a distributed deformation model. Our ongoing geodetic, paleomagnetic, and structural measurements—together with geodetic measurements by other groups at numerous sites flanking the creeping segment—will provide the basis for a strong future test.

ACKNOWLEDGMENTS

We are grateful to B. Eade, P. Duncan, P. Martin, B. Petrovich, and B. Whitney for access to critical localities. We thank J. Davis, S. Giorgis, N. Lord, and B. Unger for their assistance in the field. J. Langbein was instrumental in locating the original alignment-array data. We also thank D. Douglas, D. Rodman, A. Snyder, and J. Starmer for their assistance, as well as W. Prescott and an anonymous reviewer for their helpful comments. This material is based upon work supported by a National Science Foundation (NSF) Graduate Research Fellowship (Titus) and NSF grant EAR-0208038.

REFERENCES CITED

Altamimi, Z., Sillard, P., and Boucher, C., 2002, ITRF2000: A new release of the International Terrestrial Reference Frame for earth science applications: Journal of Geophysical Research, v. 107, no. 10, doi: 10.1029/2001JB000561.

Argus, D.F., and Gordon, R.G., 2001, Present tectonic motion across the Coast Ranges and San Andreas fault system in central California: Geological Society of America Bulletin, v. 113, p. 1580–1592.

Burford, R.O., and Harsh, P.W., 1980, Slip on the San Andreas fault in central California from alinement array surveys: Seismological Society of America Bulletin, v. 70, p. 1233–1261.

Clark, J.C., Brabb, E.E., Greene, H.G., and Ross, D.C., 1984, Geology of Point Reyes Peninsula and implications for San Gregorio fault history, *in* Crouch, J.K., and Bachman, S.B., eds., Tectonics and sedimentation along the California margin: Pacific Section, Society of Economic Paleontologists and Mineralogists, Field Trip Guidebook, p. 67–85.

Dibblee, T.W., Jr., 1976, The Rinconada and related faults in the southern Coast Ranges, California, and their tectonic significance: U.S. Geological Survey Professional Paper, 55 p.

Hall, N.T., Hunt, T.W., and Vaughan, P.R., 1994, Holocene behavior of the San Simeon fault zone, south-central coastal California, *in* Alterman, I.B., et al., eds., Seismotectonics of the central California Coast Ranges: Geological Society of America Special Paper 292, p. 167–189.

Hanson, K.L., and Lettis, W.R., 1994, Estimated Pleistocene slip rate for the San Simeon fault zone, south-central coastal California, *in* Alterman, I.B., et al., eds., Seismotectonics of the central California Coast Ranges: Geological Society of America Special Paper 292, p. 133–150.

Heflin, M., Beriger, W., Blewitt, G., Freedman, A.P., Hurst, K., Lichten, S., Lindqwister, U.J., Vigue, Y., Webb, F., Yunch, T.P., and Zumberge, J., 1992, Global geodesy using GPS without fiducial sites: Geophysical Research Letters, v. 19, p. 131–134.

Hill, D.P., Eaton, J.P., and Jones, L.M., 1990, Seismicity, 1980–1986, *in* Wallace, R.E., ed., The San Andreas fault system, California: U.S. Geological Survey Professional Paper 1515, p. 115–152.

Jamison, W.R., 1991, Kinematics of compressional fold development in convergent wrench terranes: Tectonophysics, v. 190, p. 209–232.

King, N.E., Segall, P., and Prescott, W., 1987, Geodetic measurements near Parkfield, California, 1959–1984: Journal of Geophysical Research, v. 92, p. 2747–2766.

Lienkaemper, J.J., Borchardt, G., and Lisowski, M., 1991, Historic creep rate and potential for seismic slip along the Hayward fault, California: Journal of Geophysical Research, v. 96, p. 18,261–18,283.

Lisowski, M., and Prescott, W.H., 1981, Short-range distance measurements along the San Andreas fault system in central California, 1975 to 1979: Seismological Society of America Bulletin, v. 71, p. 1607–1624.

Lisowski, M., Savage, J.C., and Prescott, W.H., 1991, The velocity field along the San Andreas fault in central and southern California: Journal of Geophysical Research, v. 96, p. 8369–8389.

McLaren, M.K., and Savage, W.U., 2001, Seismicity of south-central coastal California: October 1987 through January 1997: Seismological Society of America Bulletin, v. 91, p. 1629–1658.

Page, B.M., Thompson, G.A., and Coleman, R.G., 1998, Late Cenozoic tectonics of the central and southern Coast Ranges of California: Geological Society of America Bulletin, v. 110, p. 846–876.

Prescott, W.H., Savage, J.C., Svarc, J.L., and Manaker, D., 2001, Deformation across the Pacific–North America plate boundary near San Francisco, California: Journal of Geophysical Research, v. 106, p. 6673–6682.

Savage, J.C., and Burford, R.O., 1973, Geodetic determination of relative plate motion in central California: Journal of Geophysical Research, v. 78, p. 832–845.

Schulz, S.S., 1989, Catalog of creepmeter measurement in California from 1966 through 1988: U.S. Geological Survey Open-File Report 89-065, 193 p.

Schulz, S.S., Mavko, G.M., Burford, R.O., and Stuart, W.D., 1982, Long-term fault creep observations in central California: Journal of Geophysical Research, v. 87, p. 6977–6982.

Segall, P., and Harris, R., 1987, Earthquake deformation cycle on the San Andreas fault near Parkfield, California: Journal of Geophysical Research, v. 92, p. 10,511–10,525.

Sieh, K.E., and Jahns, R.H., 1984, Holocene activity of the San Andreas fault at Wallace Creek, California: Geological Society of America Bulletin, v. 95, p. 883–896.

Teyssier, C., and Tikoff, B., 1998, Strike-slip partitioned transpression of the San Andreas fault system: A lithospheric-scale approach, *in* Holdsworth, R.E., et al., eds., Continental transpressional and transtensional tectonics: Geological Society [London] Special Publication 135, p. 143–158.

Tikoff, B.T., and Peterson, K., 1998, Physical experiments of transpressional folding: Journal of Structural Geology, v. 20, p. 661–672.

Toppozada, T.R., Branum, D.M., Reichle, M.S., and Hallstrom, C.L., 2002, San Andreas fault zone, California: M ≥ 5.5 earthquake history: Seismological Society of America Bulletin, v. 92, p. 2555–2601.

Yamada, S., 1999, The role of soil creep and slope failure in the landscape evolution of a head water basin: Field measurements in a zero order basin of northern Japan: Geomorphology, v. 28, p. 329–344.

Zumberge, J.R., Heflin, M.B., Jefferson, D.C., Watkins, M.M., and Webb, F.H., 1997, Precise point positioning for the efficient and robust analysis of GPS data from large networks: Journal of Geophysical Research, v. 102, p. 5005–5017.

Manuscript received 13 August 2004
Revised manuscript received 19 November 2004
Manuscript accepted 23 November 2004

Printed in USA